Active Power Filter Capability of a 10 kV SiC MOSFET-Based Asynchronous Microgrid Power Conditioning System

Dingrui Li
CURENT
The University of Tennessee
Knoxville, TN, USA
dli35@vols.utk.edu

Cheng Nie
CURENT
The University of Tennessee
Knoxville, TN, USA
cnie@utk.edu

Xingxuan Huang
CURENT
The University of Tennessee
Knoxville, TN, USA
xhuang36@vols.utk.edu

Min Lin
CURENT
The University of Tennessee
Knoxville, TN, USA
mlin12@vols.utk.edu

Fred Wang
CURENT
The University of Tennessee
Oak Ridge National Laboratory
Knoxville, TN, USA
fred.wang@utk.edu

Leon M. Tolbert
CURENT
The University of Tennessee
Knoxville, TN, USA
tolbert@utk.edu

***Abstract*—Asynchronous microgrid (ASMG) with a power conditioning system (PCS) is a promising solution for future microgrids (MGs). High voltage (HV, >3.3 kV) SiC device-based PCS is becoming more and more popular in the ASMG PCS implementation. PCS with HV SiC MOSFETs can realize higher control frequencies with lower losses to bring numerous system-level benefits, which have not been fully investigated in the existing literature. In this paper, the active power filtering (APF) capability of the HV SiC-based PCS for both grid and MG power quality improvement is discussed and demonstrated. A harmonic impedance-based APF algorithm is proposed for MG-side PCS. The PCS APF functions are demonstrated on a 10 kV SiC MOSFET-based PCS prototype with the modular multi-level converter (MMC) topology to 19th-order harmonic currents.**

Keywords—Asynchronous microgrid, high voltage SiC MOSFET, active power filter

I. Introduction

ASMG is a novel MG concept for future distribution grids. In an ASMG, the MG interfaces with the main grid through a back-to-back connected medium voltage (MV) PCS, as shown in Fig. 1 [1]. The PCS can decouple the dynamics of the main grid and MG, resulting in better transition performances [2], fault isolation [3], etc. As the core component of an ASMG, PCS implementation is critical. The Si-based PCS is lossy and suffers from a low switching frequency, increasing the system size and power losses, which limits the ASMG adoption. Recently, due to the development of HV SiC devices, the HV SiC-based converter is becoming a promising candidate for the implementation of the ASMG PCS, which can realize a much higher switching frequency with lower losses to benefit the PCS size and efficiency [4-8]. Moreover, the SiC-based PCS not only leads to converter-level benefits but also results in more system-level benefits like potential stability enhancement [9]. However, system-level benefits from the HV SiC devices have not been fully investigated in the existing literature.

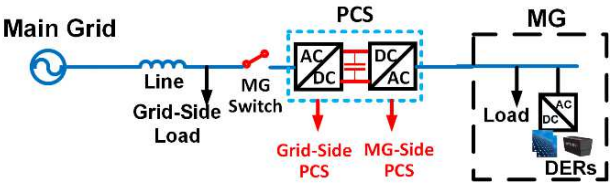

Fig. 1. ASMG structure.

In this paper, the APF capability of the SiC-based PCS is demonstrated. The PCS can serve as an APF for both the grid and MG to improve the power quality of the whole system. However, the APF capability of a Si-based PCS is limited by the low switching frequency. For a SiC-based PCS, the higher switching frequency leads to a higher filtering frequency range so that the PCS APF capability can be further explored. The harmonic filtering capabilities of both grid-side PCS and MG-side PCS are discussed first. Then the control algorithms of harmonic filtering are introduced for both grid-side and MG-side PCS, specifically, a harmonic impedance-based APF strategy is proposed for the MG-side PCS. Finally, the proposed algorithms are demonstrated on a 10 kV SiC MOSFET-based PCS with a MMC topology.

The structure of this paper is organized as follows: Section II introduces the harmonic load in an ASMG and discusses the harmonic current filtering capability of the PCS in different

operation modes; Section III covers the APF control algorithms for the MMC-based PCS; experimental results are provided in Section IV; Section V concludes.

II. ASMG Concept and SiC-Based PCS APF Capability

A. ASMG Concept

In an AMSG, the PCS operation condition changes with the MG modes. In the grid-connected mode, the grid-side PCS works in the grid-following (GFL) mode to regulate MV dc voltage, and the MG-side PCS is in grid-forming (GFM) mode to form the MG voltage and frequency as well as support the load in the MG. In the islanded mode, the grid-side PCS is shut down; the MG-side PCS changes its operation mode to GFL mode to control the MV dc-link voltage and potentially compensate reactive power of the MG.

B. Harmonic Load in an ASMG

According to IEEE Std 1159-2019 [10], electronic-interfaced equipment is the main contributor to grid harmonics. Electronic-interfaced equipment includes loads that have diode bridges and loads that have pulse-width modulated inverters, where the former type usually leads to much larger current harmonics than the latter one because pulse-width modulated inverters usually have passive filters to limit the harmonic current injection to the grid.

Diode bridges usually serve as rectifiers, which can be modeled as current sources in the harmonic circuit [10]. Large three-phase rectifiers like front-end rectifiers can contribute to numerous harmonic currents, of which the harmonic currents can be written as:

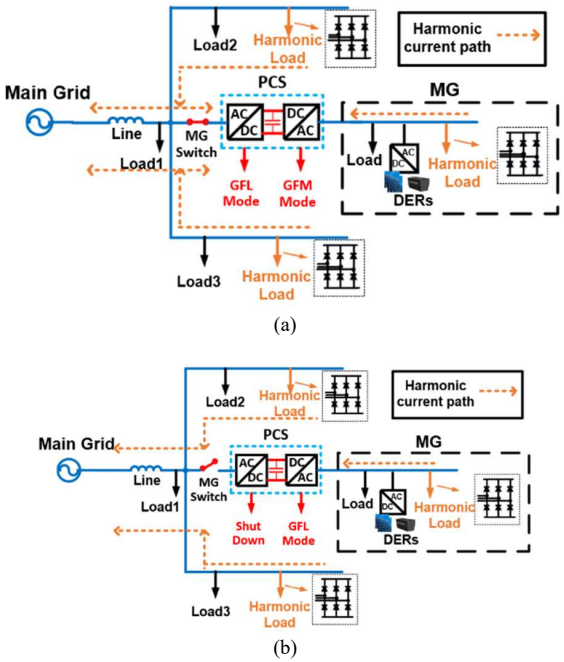

Fig. 2. ASMG APF capability: (a) grid-connected mode; (b) islanded mode.

$$\begin{cases} i_{ah}(t) = I_h \cos(h\omega t + \theta_h) \\ i_{bh}(t) = I_h \cos(h\omega t + \theta_h - h\frac{2\pi}{3}) \\ i_{ch}(t) = I_h \cos(h\omega t + \theta_h + h\frac{2\pi}{3}) \end{cases} \quad (1)$$

where h is the harmonic order. In power grids, odd-order harmonics are the main harmonics [10-11]. Therefore, the three-phase harmonic three-phase angles are:

$$\begin{cases} Postive\ sequence\ order, & h = 3m + 1 \\ Negative\ sequence\ order, & h = 3n + 2 \\ Zero\ sequence\ order, & h = 3n \end{cases} \quad (2)$$

where m is an even integer; n is an odd integer. Positive sequence order means the phase angle of phase b is $-\frac{2\pi}{3}$ and the phase angle of phase c is $\frac{2\pi}{3}$; negative sequence order means the phase angle of phase b is $\frac{2\pi}{3}$ and the phase angle of phase c is $-\frac{2\pi}{3}$; zero sequence order means three phase angles are the same. In this paper, the compensation of the zero sequence harmonic currents will not be discussed.

C. SiC-Based PCS APF Capability

1) SiC-Based PCS Harmonic Decoupling and Filtering

Harmonic current is a main concern for the grid power quality. In the grid-connected mode, as shown in Fig. 2 (a), both sides of the PCS have harmonic loads. The grid-side PCS will regulate a stable dc-link voltage so that the grid-side and MG-side harmonic currents can be decoupled. The grid-side harmonic current may flow into the grid-side PCS, meaning that the grid-side PCS may compensate for the grid-side harmonic currents to benefit the grid power quality. Meanwhile, on the MG side, harmonic current will be fully provided by the MG-side PCS and distributed energy resources (DERs) in both grid-connected and islanded operation modes. As a result, the MG-side PCS can compensate for the MG-side harmonic currents.

However, a Si-based PCS features low control and switching frequency (several kilohertz) [12], meaning that it is difficult for a Si-based PCS to filter relatively higher-order harmonics like thirteenth (13^{th})-order or seventeenth (17^{th})-order harmonics. Note that the Si-based PCS can also achieve high control frequency by increasing the PCS voltage level number such as replacing a five-level topology with a seven-level topology, however, this solution will highly increase the cost and control complexity of the PCS. For a SiC-based PCS, the control frequency of the PCS can be up to 10 kHz or higher with smaller losses and control complexity compared to the Si-based PCS [13]. Therefore, the SiC-based PCS can have more flexibility for APF function to benefit the whole ASMG.

2) Grid-Side PCS APF Capability

The harmonic equivalent circuit of the ASMG in the grid-connected mode is shown in Fig. 3(a). The grid lines are viewed as harmonic impedances, which are written as [14]:

$$Z_{Line}^{h} = h2\pi f_l L_{Line} + R_{line} \quad (3)$$

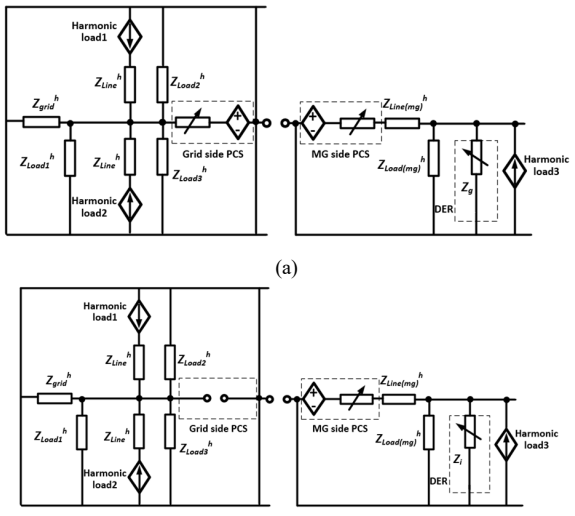

Fig. 3. ASMG harmonic equivalent circuit: (a) grid-connected mode; (b) islanded mode.

where L_{line} and R_{Line} are the line inductance and resistance; f_l is the fundamental frequency; h is the harmonic order. The grid usually does not have a harmonic source; therefore, the equivalent circuit is its harmonic impedance. Loads may also provide paths for harmonic currents, therefore, the loads in the harmonic circuit are also modeled as harmonic impedances.

The DERs are connected to the MG through their interface inverters, which regulate output power in the grid-connected model and control output voltage in the islanded mode. A DER inverter usually focuses on the control of fundamental components. As a result, in the harmonic circuit, it can be modeled as an impedance. Note that if a DER has specific harmonic control, then in the harmonic circuit, it can be modeled as an impedance plus harmonic voltage source (harmonic voltage control) or a harmonic current source (harmonic current control).

The grid-side and MG-side PCS can both be modeled as a controlled voltage source plus a variable impedance. The inverter's harmonic performance is determined by its rating and control strategy. For the grid-side PCS, the PCS is only designed for supporting the targeted MG which is only a small part of the whole distribution grid. As a result, the grid-side PCS rating is not sufficient to compensate for all the harmonic currents in the main grid. Therefore, the grid-side PCS can either compensate the harmonic current of one feeder or partially compensate the grid harmonic current based on grid requirements [15].

3) MG-Side PCS APF Capability

On the MG side, the harmonic current distribution is simpler compared to the distribution of the grid side. The harmonic current can potentially flow into the load, DER, and PCS, which may affect the operation of loads and DERs. In the grid-connected mode, the MG-side PCS serves as the source of the MG. Considering the potential power fluctuation of DERs, it should be able to support all the load even when there is no DER generation. Therefore, the MG-side PCS has a sufficient rating to compensate for all the harmonic currents, which can avoid additional APF installation in the MG.

III. PCS APF Control Algorithms

A. Control Function Architecture

As shown in Fig. 4, the PCS control includes the system-required control and topology-required control. The system-required control contains the PCS operation control to support the ASMG operation and the APF control is to benefit the main grid and the MG. The topology-required control is designed to satisfy the PCS topology requirement. For the MMC-based PCS, the PCS topology-required control includes the second-order arm circulating current and modulation. The detailed discussion and descriptions of the PCS operation control and topology-required control are covered in [16] and [17]. The APF function is concentrated on in this paper.

B. APF Control Algorithms

1) APF Function of Grid-Side PCS

In the grid-connected mode, the grid-side PCS regulates the dc voltage and outputs reactive power to the grid. For the APF function, the grid-side PCS cannot compensate all the grid-side harmonic currents, therefore, the PCS will realize the harmonic current filtering based on the received grid requirements. Note that the received harmonic current requirements should be within the compensation capability of the grid-side PCS. If the requirement is greater than the maximum rating of the grid-side PCS rating, the compensation will be limited to the maximum rating of the PCS.

As shown in Fig. 5, the received harmonic current references and measured PCS current currents are transformed into harmonic dq coordinates and the harmonic current control is realized in dq coordinates. According to (2), when the harmonic phase order is positive sequence order, the positive sequence dq transformation will be conducted, where the transformation matrix is:

$$T_{dq}^{1} = \sqrt{\frac{2}{3}}\begin{bmatrix} \cos\omega t & \cos\left(\omega t - \frac{2\pi}{3}\right) & \cos\left(\omega t + \frac{2\pi}{3}\right) \\ -\sin\omega t & -\sin\left(\omega t - \frac{2\pi}{3}\right) & -\sin\left(\omega t + \frac{2\pi}{3}\right) \end{bmatrix} \quad (4)$$

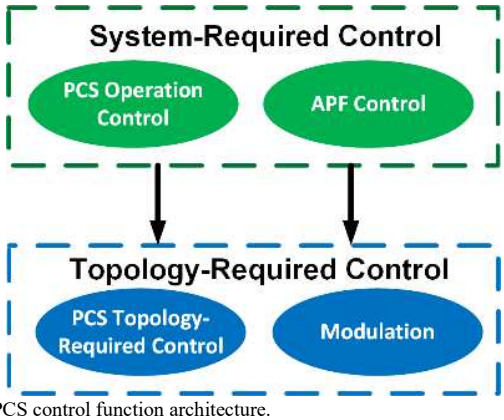

Fig. 4. PCS control function architecture.

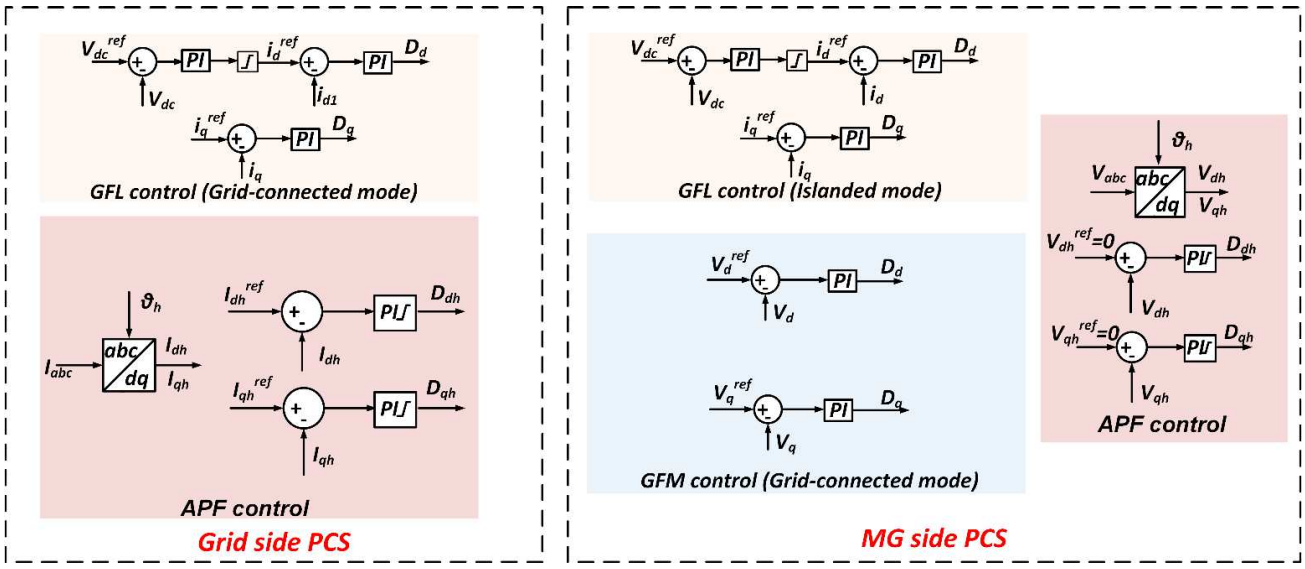

Fig. 5. ASMG APF control algorithms.

Meanwhile, when the harmonic phase order is negative sequence order, the negative sequence *dq* transformation will be conducted, the transformation matrix is:

$$T_{dq}^{2}=\sqrt{\frac{2}{3}}\begin{bmatrix}\cos\omega t & \cos\left(\omega t+\frac{2\pi}{3}\right) & \cos\left(\omega t-\frac{2\pi}{3}\right)\\ \sin\omega t & \sin\left(\omega t+\frac{2\pi}{3}\right) & \sin\left(\omega t-\frac{2\pi}{3}\right)\end{bmatrix} \quad (5)$$

Moreover, after the harmonic *dq* transformation, the fundamental frequency PCS current will be transformed to be higher orders. For example, when the fifth-order harmonic *dq* transformer is conducted, the fifth-order harmonic current will be transformed into dc components while the fundamental current will be transformed to be fourth-order or six-order components. As a result, the control of the fundamental components can be potentially affected. To avoid this issue, in this paper, the control bandwidths of the proportional-integral (*PI*) controllers in the harmonic current control loop are designed to be lower than 60 Hz so that the *PI* controllers will not have enough gain at the fundamental frequency components in the harmonic *dq* coordinates so that the harmonic control will not affect the control of fundamental frequency components.

2) APF Function of MG-Side PCS

For the MG-side PCS, it works as an APF in both operation modes. Since the PCS has a sufficient rating to compensate for all the harmonic currents, the harmonic current compensation can be realized by regulating the output impedance to be zero. When the harmonic impedance is zero, the harmonic current can flow into the PCS rather than loads or DERs. As shown in Fig. 6, when the MG-side PCS achieves a zero harmonic impedance, in the harmonic circuit, the harmonic current distribution is only determined by the impedance relationships among load impedance, DER impedance, and line impedances. Meanwhile, the ASMG is usually small, meaning that the line is short. The line impedances can be neglected compared to the DER and load impedances. Therefore, the harmonic currents will be provided by the PCS. Furthermore, as shown in Fig. 5, to achieve zero harmonic impedance, one direct way is to regulate the harmonic voltage to be zero. The control is also implemented in *dq* coordinates in both grid-connected and islanded modes.

IV. Experimental Demonstration

A. System Setup

A 10 kV SiC MOSFET-based, 5-level MMC is adopted as the PCS for a MV ASMG [13]. As shown in Fig. 7, a test setup is proposed to verify the APF functions for both sides of the PCS, simultaneously. In the testing setup, the grid-side PCS is connected to the load to serve as a harmonic source to output harmonic currents to the load, and the MG-side PCS will work as an APF to compensate for all the harmonic currents in the MG. In the testing setup, the MG-side PCS operates in the GFM mode to support the load.

The hardware setup is shown in Fig. 8 and the system parameters are summarized in Table I. In the testing setup, the PCS will operate at 12 kV dc-link voltage and 6.8 kV ac voltage. The control bandwidth of the PCS is 10 kHz. The load is

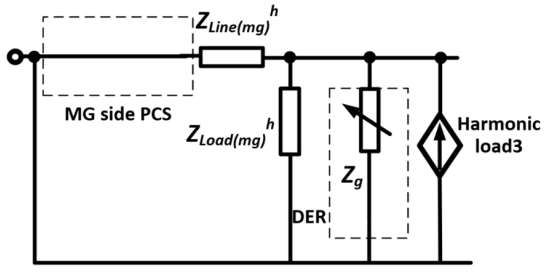

Fig. 6. MG-side harmonic circuit when PCS harmonic impedance is regulated to be zero.

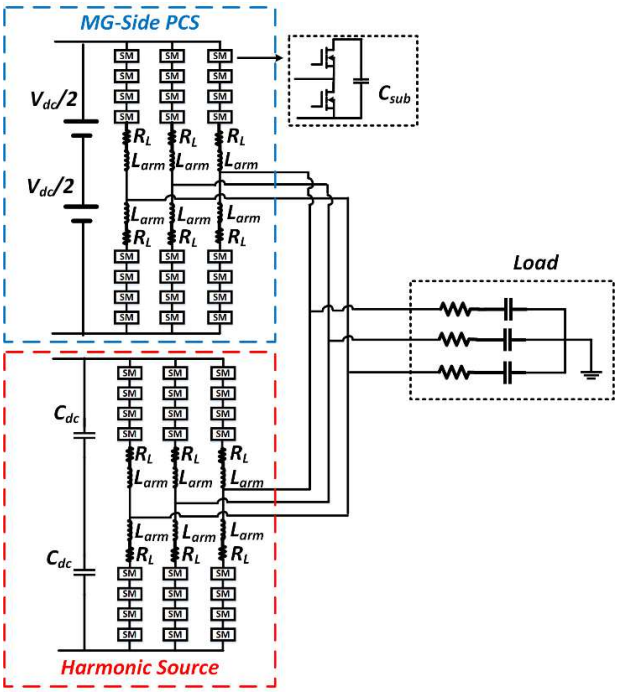

Fig. 7. MG-side PCS APF testing setup.

Fig. 8. PCS APF testing hardware setup.

TABLE I. TESTING SETUP PARAMETERS

Parameters	Values
DC-link voltage (V_{dc})	12 kV
AC line voltage (V_{ac})	6.8 kV
Load (R_{load} and C_{load})	R_{load}=246 Ω, C_{load}=1.25 uF
Line frequency (f_l)	60 Hz
Arm inductor (L and R_L)	L=90 mH, R_L= 5 mΩ
Control frequency (f_c)	10 kHz

composed of resistors and capacitors. The load harmonic impedance can be written as:

$$Z_{load}^{h} = R_{Load} + \frac{1}{jh2\pi f_l C_{Load}} \quad (6)$$

where *h* is the harmonic order. When the order of the harmonic current is increased, the harmonic impedance of the load will be decreased. As a result, more harmonic currents will flow into the load. Detailed information on the MMC-based PCS can be found in [13] and [18].

B. *Experimental Testing Results*

In the experimental testing, the filtering of the 13th-order, 17th-order, and nineteenth (19th)-order harmonic currents are tested. The testing results are shown in Fig. 9, Fig. 10, and Fig. 11, respectively.

According to Fig. 9 (a), when the APF is not applied, the harmonic current will flow into both the PCS and the load. The FFT results indicate that the harmonic current of the load is

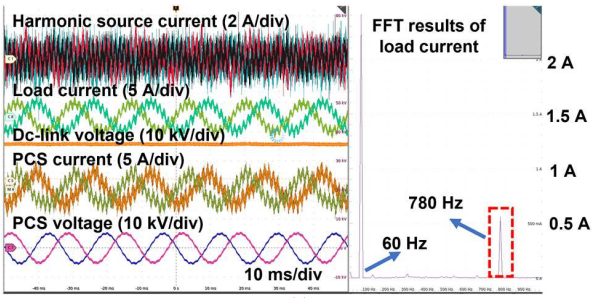

(a)

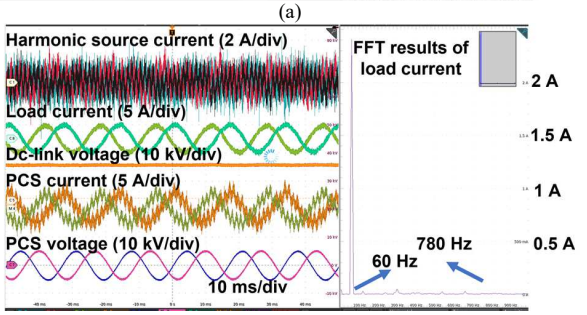

(b)

Fig. 9. Testing results for APF function of 13th-order harmonic currents: (a) without APF control; (b) with APF control.

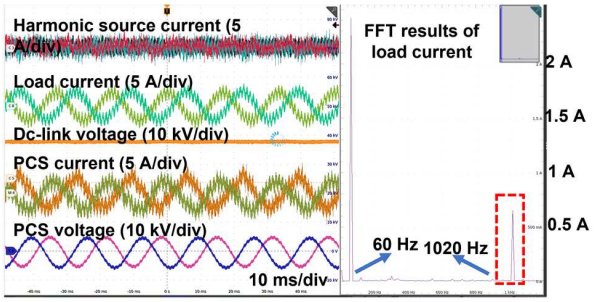

(a)

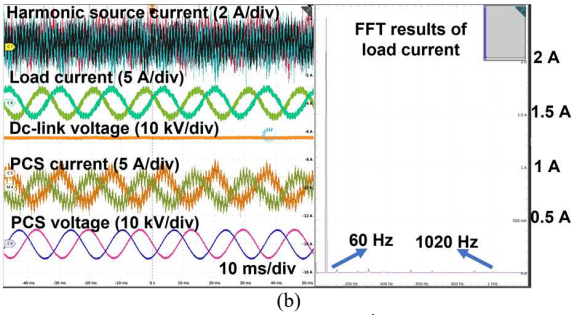

(b)

Fig. 10. Testing results for APF function of 17th-order harmonic currents: (a) without APF control; (b) with APF control.

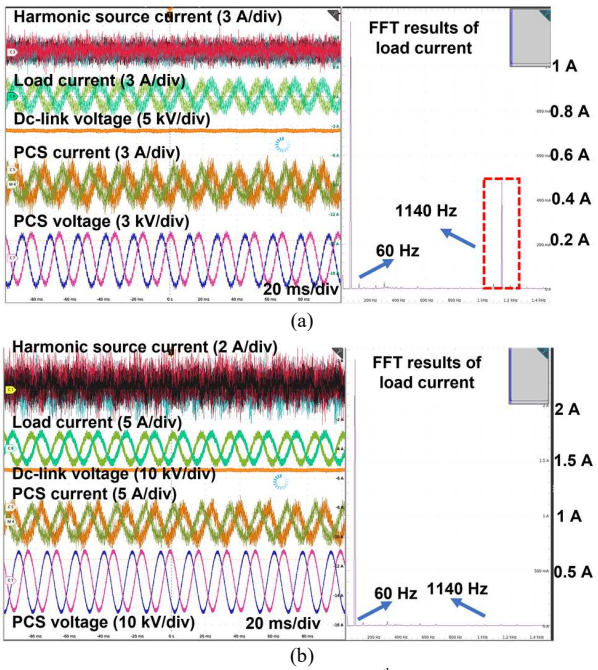

Fig. 11. Testing results for APF function of 19th-order harmonic currents: (a) without APF control; (b) with APF control.

mainly 13th-order, showing that the grid-side PCS (harmonic current source) can output a required harmonic current. When the APF function is applied to the PCS as shown in Fig. 9 (b), the 13th-order harmonic current of the load is compensated (less than 0.05 A), and all the harmonic currents flow into the PCS.

Similarly, in Fig. 10 and Fig. 11, 17th-order and 19th-order harmonic currents are generated by the grid-side PCS. According to Fig. 10 (a) and Fig. 11 (a), when the APF function of the PCS is not enabled, the harmonic current will flow into the load. When the APF function is enabled, the PCS can compensate for both the 17th-order and 19th-order harmonic currents and the load will not be impacted by the harmonics (harmonic current is less than 0.05 A). Note that, for the 19th-order harmonic current, since the harmonic impedance of the capacitor load is small, the majority of the harmonic current will flow into the capacitor. In order to avoid the potential damage of the capacitor, when PCS APF is not applied, the dc voltage is only 6 kV. When the PCS APF is applied, the dc voltage can still operate to 12 kV. Overall, the testing results can demonstrate the APF capability of both grid-side PCS and MG-side PCS.

Moreover, during the testing, it is demonstrated that the SiC-based PCS is able to filter the harmonic currents up to 19th-order (1140 Hz). It is very difficult for a Si-based PCS to achieve the same harmonic order because a Si-based PCS usually has a low control frequency. Therefore, the improvement of the APF capability from the HV SiC MOSFETs can be demonstrated.

V. Conclusion

In this paper, the APF capability of a SiC-based ASMG PCS is analyzed and verified with experimental results. Compared to the Si-based PCS, the SiC-based PCS can cover significantly higher harmonic orders to further benefit the grid and MG power quality. For the main grid, the grid-side PCS filters the harmonics based on grid-side requirements. For the MG-side PCS, a harmonic impedance-based approach is proposed to filter all the MG load harmonics by regulating the harmonic impedance to zero. By implementing this approach, the MG-side PCS can realize the APF capability without additional current sensors or communications. The testing results prove that the SiC-based PCS can achieve the APF function up to 19th-order harmonic currents, demonstrating a novel power quality benefit enabled by the SiC-based MV converter.

Acknowledgment

This work was supported primarily by U.S. DOE PowerAmerica program at North Carolina State University. The authors would like to thank Southern Company, EPB, and EPC Power for their support of the project. The authors acknowledge Powerex for helping package the 10 kV SiC MOSFETs. This work made use of the Engineering Research Center Shared Facilities supported by the Engineering Research Center Program of the National Science Foundation and DOE under NSF award number EEC-1041877 and the CURENT Industry Partnership Program.

References

[1] M. Barnes and P. Binduhewa, "Asynchronous interconnection of a microgrid," in *CIRED Seminar*, Frankfurt, Germany, 2008, pp. 64-68.

[2] J.-D. Park, J. Candelaria, L. Ma, and K. Dunn, "DC ring-bus microgrid fault protection and identification of fault location," *IEEE Transactions on Power Delivery,* vol. 28, pp. 2574-2584, 2013.

[3] J. Wang, N. C. P. Chang, X. Feng, and A. Monti, "Design of a generalized control algorithm for parallel inverters for smooth microgrid transition operation," *IEEE Transactions on Industrial Electronics,* vol. 62, pp. 4900-4914, 2015.

[4] N. He, M. Chen, J. Wu, N. Zhu, and D. Xu, "20-kW zero-voltage-switching SiC-MOSFET grid inverter with 300 kHz switching frequency," *IEEE Transactions on Power Electronics*, vol. 34, no. 6, pp. 5175-5190, June 2019.

[5] S. Parashar, A. Kumar, and S. Bhattacharya, "High power medium voltage converters enabled by high voltage SiC power devices," in *Proc. International Power Electronics Conference (ECCE Asia)*, 2018, pp. 3993-4000.

[6] S. Madhusoodhanan *et al*., "Solid-state transformer and MV grid tie applications enabled by 15 kV SiC IGBTs and 10 kV SiC MOSFETs based multilevel converters," *IEEE Transactions on Industry Applications*, vol. 51, no. 4, pp. 3343-3360, July-Aug. 2015.

[7] X. Huang, S. Ji, J. Palmer, L. Zhang, L. M. Tolbert and F. Wang, "Parasitic capacitors' impact on switching performance in a 10 kV SiC MOSFET based converter," *IEEE 6th Workshop on Wide Bandgap Power Devices and Applications (WiPDA)*, Atlanta, GA, 2018, pp. 311-318.

[8] S. Belkhode, P. Rao, A. Shukla and S. Doolla, "Comparative evaluation of silicon and silicon-carbide device-based MMC and NPC converter for medium-voltage applications," *IEEE Journal of Emerging and Selected Topics in Power Electronics*, vol. 10, no. 1, pp. 856-867, Feb. 2022.

[9] D. Li *et al*., "Grid stability enhancement by a high voltage SiC MOSFET-based asynchronous microgrid power conditioning system," *in Proc.*

IEEE Applied Power Electronics Conference and Exposition (APEC), 2021, pp. 111-118.

[10] *IEEE Recommended Practice for Monitoring Electric Power Quality*, IEEE Standard 1159-2019, Aug. 2019.

[11] J. Yu, X. Lin, D. Song, R. Yu, Y. Li and M. Su, "Harmonic instability and amplification for grid-connected inverter with voltage harmonics compensation considering phase-locked loop," *IEEE Journal of Emerging and Selected Topics in Power Electronics*, vol. 8, no. 4, pp. 3944-3959, Dec. 2020.

[12] D. Krug, S. Bernet, S. S. Fazel, K. Jalili and M. Malinowski, "Comparison of 2.3-kV medium-voltage multilevel converters for industrial medium-voltage drives," *IEEE Transactions on Industrial Electronics*, vol. 54, no. 6, pp. 2979-2992, Dec. 2007.

[13] S. Ji, X. Huang, L. Zhang, J. Palmer, W. Giewont*, et al.*, "Medium voltage (13.8 kV) transformer-less grid-connected DC/AC converter design and demonstration using 10 kV SiC MOSFETs," in *Proc. IEEE Energy Conversion Congress and Exposition (ECCE)*, 2019, pp. 1953-1959.

[14] Z. Wang *et al*., "Impedance-based adaptively reshaping method for enhancing nonlinear load sharing and voltage quality in islanded microgrids with virtual synchronous generator," *IEEE Transactions on Smart Grid*, vol. 13, no. 4, pp. 2568-2578, July 2022.

[15] C. Lam, W. Choi, M. Wong and Y. Han, "Adaptive DC-link voltage-controlled hybrid active power filters for reactive power compensation," *IEEE Transactions on Power Electronics*, vol. 27, no. 4, pp. 1758-1772, April 2012.

[16] D. Li, S. Ji, X. Huang, J. Palmer, F. Wang and L. M. Tolbert, "Controller development of an asynchronous microgrid power conditioning system (PCS) converter considering grid requirements," in *Proc. IEEE Applied Power Electronics Conference and Exposition (APEC)*, 2020, pp. 616-621.

[17] S. Ji, L. Zhang, X. Huang, J. Palmer, F. Wang and L. M. Tolbert, "A novel voltage balancing control with dv/dt reduction for 10-kV SiC MOSFET-based medium voltage modular multilevel converter," *IEEE Transactions on Power Electronics*, vol. 35, no. 11, pp. 12533-12543, Nov. 2020

[18] D. Li, X. Huang, S. Ji, C. Nie, F. Wang and L. M. Tolbert, "Controller design and implementation of a medium voltage (13.8 kV) modular multi-level converter for asynchronous microgrids," in *Proc. IEEE Energy Conversion Congress and Exposition (ECCE)*, 2020, pp. 4642-4648.